Title	Stress conditions inferable from modern magnitudes: development of a model of fault maturity
Author	**George L. Choy**, U. S. Geological Survey, Denver, CO 80215, E-mail: choy@usgs.gov
Version	August 2011; **DOI: 10.2312/GFZ.NMSOP-2_IS_3.5**

1 Introduction

Although Me and Mw are magnitudes that describe the size of an earthquake, they are not equivalent. Me, being derived from velocity power spectra, is a measure of the radiated energy in the form of seismic waves and, thus, of the seismic potential for damage to anthropogenic structures. Mw, being derived from the low-frequency asymptote of displacement spectra, is physically related to the final static displacement of an earthquake. As seen in the Me-Mw plot of global earthquakes from 1987-2009 (Figure 1), for any given Mw, the corresponding Me may vary by as much as an entire magnitude unit and vice versa.

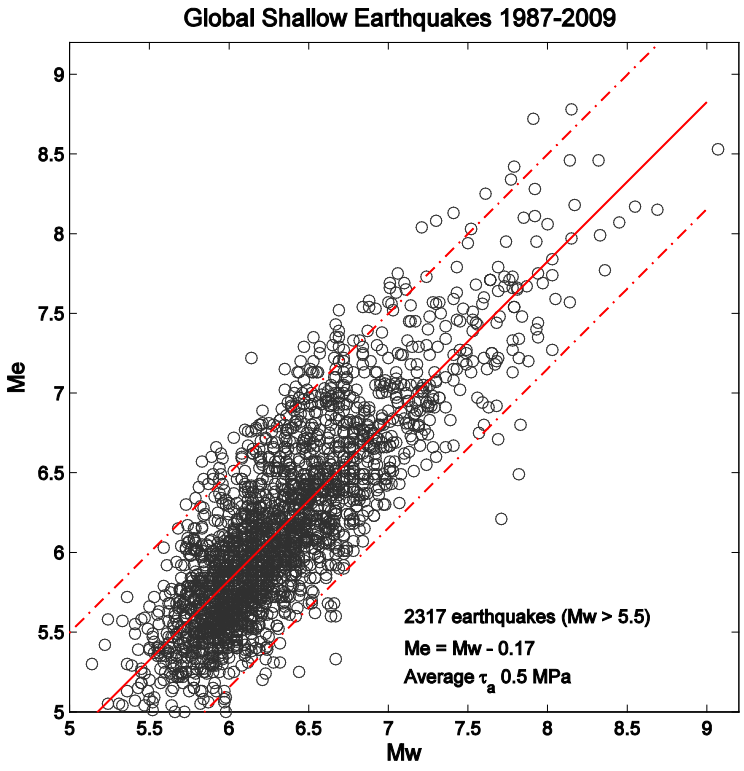

Figure 1 Me-Mw for global shallow (depth < 70 km) earthquakes with magnitude greater than about 5.5. Me are taken from the USGS/NEIC source parameters catalog which has included direct computation of radiated energy Es since 1987. Mw are taken from the global Centroid Moment Tensor (gCMT) catalog. The least-squares linear regression with an assumed slope of one (solid line) yields a global average apparent stress for earthquakes of 0.5 MPa. But the 95% spread about the mean (indicated by the dashed lines) shows that for any given Mw, Me scatters about one-half a magnitude unit above and below the mean value, with some outliers up to one magnitude unit. No single empirical formula can adequately represent such a spread.

Events with anomalously high Me relative to Mw should have greater potential for seismic damage than those earthquakes with relatively low Me. Indeed, Choy et al. (2001) [see also Table 3.2 in Chapter 3 of the first edition of the NMSOP (Bormann et al., 2002)] first demonstrated this dramatically by comparing the significantly different macroseismic effects of two earthquakes in the same epicentral region that had nearly the same Mw but had Me's differing by 1.0 unit. The objective of this Information Sheet is to demonstrate that the apparent scatter in Me-Mw is non-random. Subsets of earthquakes chosen on the basis of a specific tectonic setting, seismic region and focal-mechanism type occupy specific sectors of the Me-Mw plot. Moreover, the stress conditions unique to specific sectors can be incorporated into a model of fault maturity. Rather than be daunted by the large spread in Me-Mw, methods of estimating tsunami and seismic hazards can be enhanced by exploiting the patterns of stress conditions available from Me-Mw data.

2 Ways to measure the amount of energy released per unit moment

There are several equivalent ways to represent the radiated energy to moment ratio of an earthquake:

- Apparent stress, $\tau_a = \mu E_S / M_0$
- Scaled energy, E_S / M_0
- Slowness parameter, $\Theta = \log(E_S / M_0)$
- Differential magnitude, $\Delta M = Me - Mw$

The advantage of using apparent stress τ_a (where μ is rigidity) is that it can be related to other stresses associated with rupture (Wyss and Brune, 1968). Although the relationship between apparent stress and stress drop is model dependent, larger apparent stress generally implies larger stress drop. The dimensionless ratio E_S/M_0, often called scaled energy (Kanamori and Heaton, 2000), is independent of μ, but is slightly cumbersome to enunciate as it typically ranges from 10^{-4}-10^{-6} for teleseismically analyzable earthquakes. Taking the log of the scaled energy yields a more manageable number which Newman and Okal (1998) call the slowness parameter Θ. Another equivalent method presented here is differential magnitude ΔM, defined as the difference between the energy and moment magnitudes, Me and Mw,

$$\Delta M = Me - Mw \qquad (1)$$

From the equations for M_e and M_W, we can derive useful relationships between the various representations. We use $Mw = (2/3)(\log M_0 - 9.1)$ and $Me = (2/3)(\log E_S - 4.4)$. These forms of Mw and Me, first proposed in Chapter 3 of the NMSOP (Bormann et al., 2002) and accepted by IASPEI (2005) as standard formulas, avoid occasional rounding errors up to 0.1 m.u. which can occur in the formulas originally published by Hanks and Kanamori (1979) for Mw and by Choy and Boatwright (1995) for Me.

Between differential magnitude and scaled energy we have

$$\Delta M = (2/3) [\log (E_S/M_0) + 4.7] \qquad (2)$$

Between differential magnitude and Θ :

$$\Delta M = (2/3)\,[\Theta + 4.7]. \quad (3)$$

An important relationship between Me, M_0, and τ_a was recognized [eq. 11 of Choy and Boatwright (1995)] as $Me = (2/3)\,[\log M_0 + \log(\tau_a/\mu)] - 3.2$, which can also be written as

$$Me = (2/3)\,[\log M_0 + \log(\tau_a/\mu) - 4.8], \quad (4)$$

The constant 4.8 corresponds to the constant in the classical Gutenberg-Richter relationship $\log E_S = 4.8 + 1.5 M_S$. However, the U. S. Geological Survey´s National Earthquake Information Center accepted in its Monthly Listings of the Preliminary Determination of Epicenters July 1995 the new Choy and Boatwright (1995) constant 4.4, derived from the best fitting slope of 1.5 through directly measured log Es data vs. Ms [see Figure 4 and eq. 6 in Choy and Boatwrigth (1995)]. Replacing in eq. (4) the constant 4.8 by 4.4 yields

$$Me = (2/3)\,[\log M_0 + \log(\tau_a/\mu) - 4.4], \quad (5)$$

and when introducing therein the IASPEI (2005) standard formula $Mw = (2/3)(\log M_0 - 9.1)$

$$Me = Mw + (2/3)\,[\log(\tau_a/\mu) + 4.7]. \quad (6)$$

Equivalent relationships between Me, Mw and apparent stress were published by Bormann and Di Giacomo (2011).

The relationship between differential magnitude and apparent stress is then:

$$\Delta M = (2/3)\,[\log(\tau_a/\mu) + 4.7]. \quad (7)$$

In the Me-Mw plots that follow, Me-Mw data pairs for earthquakes based on tectonic setting and focal mechanism are fit by a least squares regression to a line with slope 1,

$$Me = Mw + c.$$

The apparent stress is related to the constant c through eq. (6). Note that in order to compute average τ_a we use μ appropriate to the source depth for each event.

3 Identifying events that radiate exceptionally high energy

To identify an earthquake as having radiated exceptionally high energy relative to its moment, we adopt the criterion of Choy and Kirby (2004) that $\tau_a > 1$ MPa or, equivalently, ΔM greater than about 0.0 (i.e., whenever $Me \geq Mw$). This criterion was derived from their global investigation of subduction-zone earthquakes, in which they found that normal-fault earthquakes occurring in high-deformation regimes were always associated with exceptionally higher energy release than other normal-fault earthquakes. Characteristics of high-deformation regimes include sharp changes in slab geometry, colliding slabs and oblique convergence at a subducting plate boundary. Less than 20% of all normal-fault earthquakes are energetic events. Figures 2 and 3 show that these high energy events occupy narrow sectors in the Me-Mw plot.

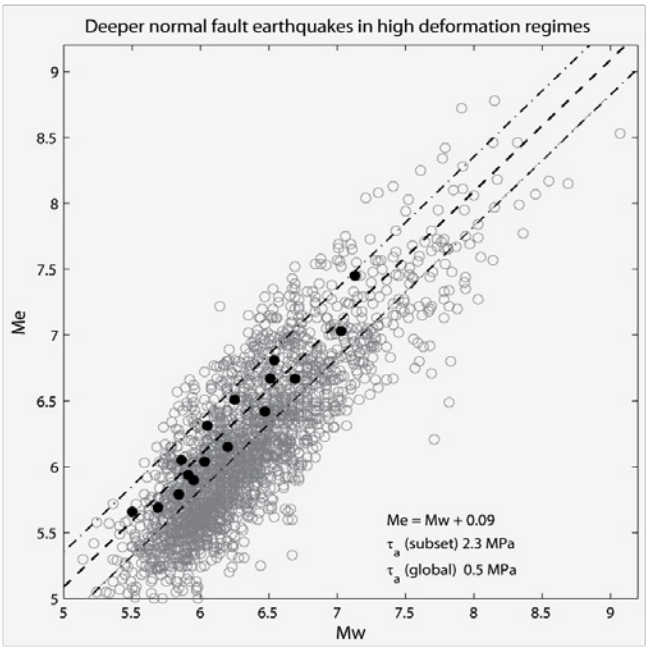

Figure 2 Me-Mw of deeper (35 km < h < 70 km) normal-fault events (solid black circles) that occur at a sharp change in slab geometry or in the deformation zone of converging but oppositely oriented slabs. These events have an average apparent stress nearly 4 times higher than the global population (gray circles).

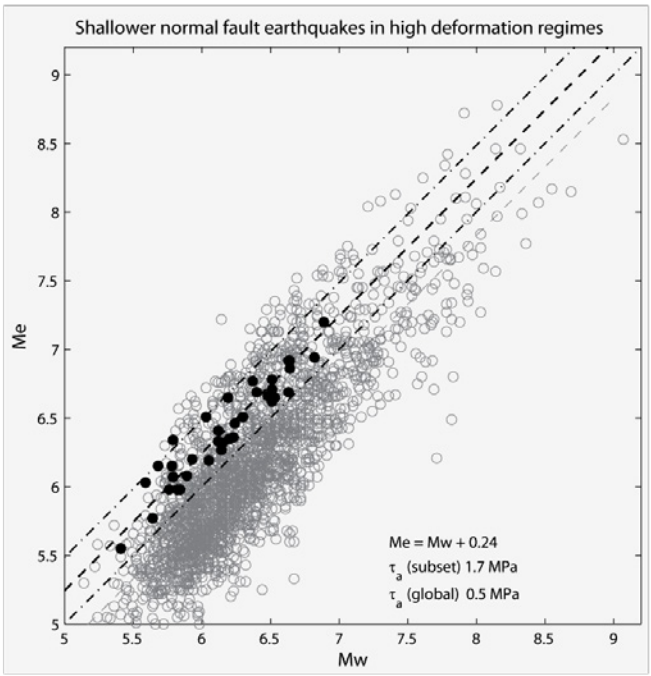

Figure 3 Me-Mw of shallower (h < 35 km) events (solid black circles) that occur intraslab and landward of the trench axis at subduction boundaries where plate convergence is oblique to the fabric of the seafloor. These events have an average apparent stress more than 3 times higher than that of the global data (gray circles).

The subset of intraoceanic strike-slip events occupies a unique sector of the Me-Mw plot. Although they constitute only 5% of the global shallow earthquakes, they have the highest average τ_a of any earthquake subset. Figure 4 plots Me-Mw for the set of strike-slip

earthquakes in the oceans (excluding subduction zones). The average τ_a for oceanic strike-slip earthquakes is about 18 times higher than the global average. At first glance this seems contrary to the original simple tenets of plate tectonic tenets, wherein strike-slip earthquakes in the oceans are thought to be dominated by the simple slippage along transform faults of weak material. Choy and McGarr (2002), however, have shown that the actual situation is far different: more oceanic strike-slip earthquakes occur in the vicinity (less than a couple of degrees) of transforms than on the transforms themselves. Far from being a simple plate boundary, ridge-transform systems are apparently the site plate boundary reorganization. The intraplate earthquakes are the consequence of fracture on new faults that result from locally intense deformation. Even the events that do occur on transforms either (1) have nodal planes not coincident with the strike of the transform; (2) occur on short-offset transform segments; or (3) occur on the inside corners of the ridge-transform intersect. These conditions also require the fracture of fresh rock or newly formed faults as the local plate boundary evolves. Moreover, the depths of nucleation of these earthquakes have been shown from broadband seismogram modeling (Choy and McGarr, 2002; Abercrombie and Ekström, 2001) to be between 5-25 km, well within the oceanic mantle. Thus, the higher strength of oceanic vs. continental mantle also contributes to the high energy release.

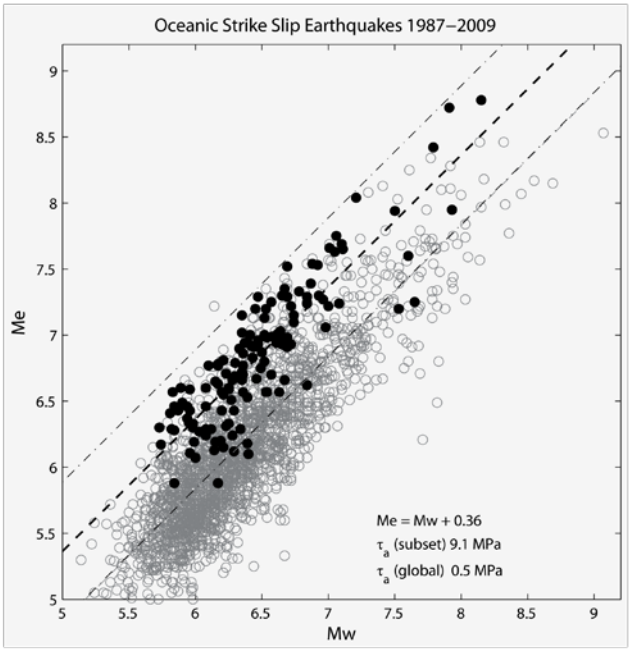

Figure 4 Me vs. Mw for the subset of 135 intraoceanic strike-slip earthquakes (dark solid circles) occurring on or near transform faults or intraplate compared to that of global earthquakes (gray circles).

4 Identifying events that radiate exceptionally low energy

To characterize an earthquake as being enervated, that is, having radiated exceptionally low energy, we adopt the criterion of Newman and Okal (1998) that its slowness parameter $\Theta < -5.5$. This is equivalent to a differential magnitude ΔM less than about -0.50. Figure 5 plots ΔM vs. M_W for all thrust earthquakes that occurred in subduction environments. The global average ΔM is -0.36. Earthquakes which radiate anomalously low energy fall below the line $\Delta M = -0.5$ (Quadrants III and IV). Quadrant IV contains the class of enervated earthquakes

with Mw > 7.5. Earthquakes in this class have been called "slow" earthquakes because of their abnormally long source durations and anomalously low radiated energy relative to seismic moment (Newman and Okal, 1998). There are only 22 such events, but virtually all of them have generated tsunamis. It should be noted that in quadrant III are another 257 earthquakes that also radiated anomalously low energy but with smaller magnitudes, Mw's < 7.5. The earthquakes in quadrants III and IV do not necessarily occur in the same seismic regions. Nor is there any obvious spatial correlation of the smaller enervated events with locations of notable slow tsunami earthquakes. This may be because patterns have not yet developed in the relatively short time for which accurate radiated energies have been available. Whether there are other tectonic, geophysical or geological connections between the large tsunamigenic earthquakes and the smaller enervated earthquakes is not known at this time and requires further research. Finally, we note that the combined population of mid-energy and enervated earthquakes (i.e., quadrants II, III and IV with $\Delta M < 0.0$) are predominantly interface thrust events for which the average τ_a a little less than 0.3 MPa. The class of subduction-interface thrust events, thus, has the lowest τ_a of any subset of earthquakes based on tectonic setting and focal mechanism.

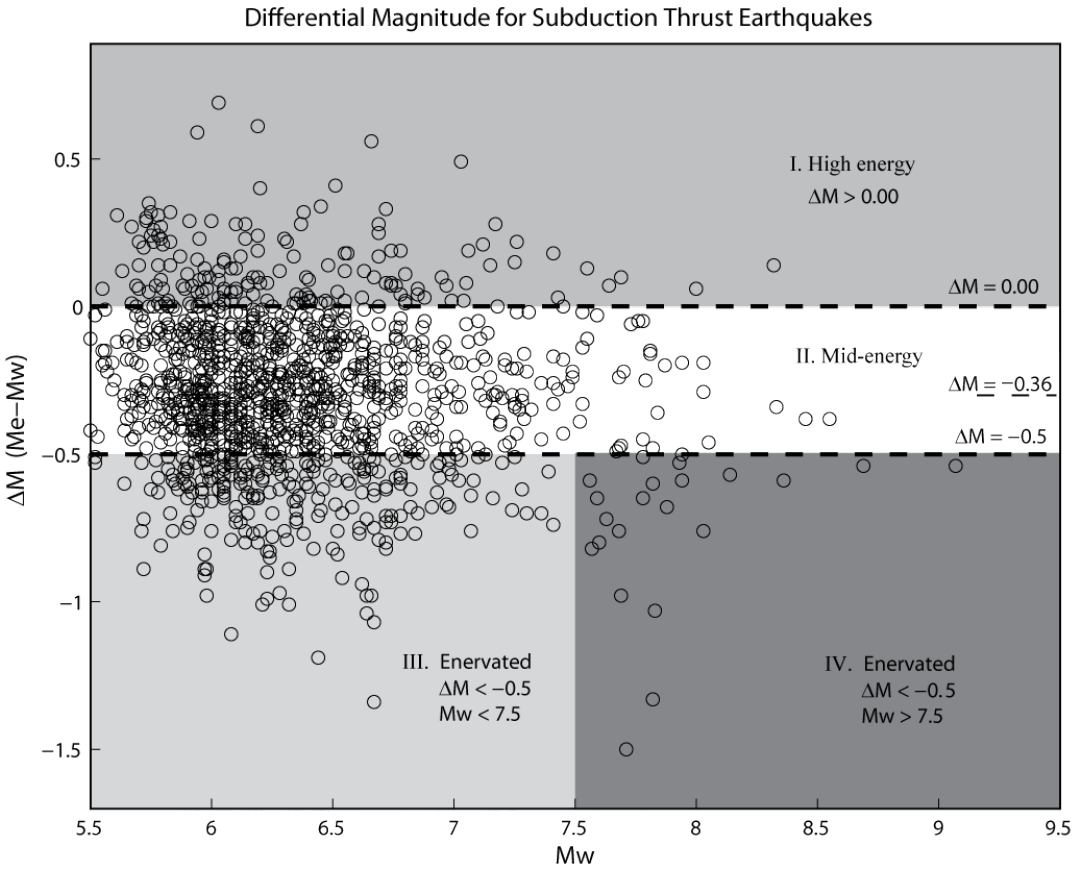

Figure 5 ΔM vs. M_W for 1306 thrust earthquakes occurring in subduction regions from 1987-2009. The global average ΔM is -0.36 (short dashed line). Earthquakes radiating anomalously low energy fall below the line $\Delta M = -0.5$ (lower dashed line). Earthquakes radiating anomalously high energy fall above the line $\Delta M = 0.0$.

Note that in quadrant I there are 163 subduction-thrust earthquakes with $\Delta M > 0.0$ which, by the criterion of our previous section, are considered to be high energy events. These

earthquakes comprise only 12% of the subduction-thrust population. They are most often found in subduction regions involving complex plate deformation (Choy and Kirby, 2009). These region types include: marine collision zones involving seamount chains or fracture zones, submerged continent-continent collisions, colliding slabs, regions of multiple plate interactions, and slab distortions. Many of these events may be intraslab based on their greater depths (compared to shallower events that are presumed to be on the subduction interface) as well as their focal mechanisms whose nodal planes are not aligned with the slab interface.

5 Development of a fault maturity model

The first three rows of Table 1 below summarize in ascending order the average apparent stresses of earthquake populations we have described, their respective tectonic settings and their dominant focal mechanism type. If we define fault maturity as the amount of offset accumulated by a fault, then we see that fault maturity is inversely related to average apparent stress. At one extreme, the least mature faults would have had little to no previously accumulated displacement and, hence, they should have maximum fault roughness. An example would be strike-slip earthquakes in oceanic lithosphere, which have the highest average τ_a of any class of earthquake. The majority of these earthquakes are either intraplate or they occur on short transforms or the inside corners of ridge-transforms (where fresh material is being ruptured). At the other extreme, the most mature faults would have large total displacements. This is typified by subduction-thrust earthquakes occurring on the frictional contact between overriding and subducting plates. Thus, the level of τ_a appears to be related to the degree to which lithosphere can sustain strain accumulation before rupturing.

Table 1 The inverse relationship between average τ_a ($<\tau_a>$ **)** of a tectonic setting and fault maturity.

$<\tau_a>$ MPa	Low → High 0.3	0.4	1.7	2.1	9.1
Subduction zone environment	Interplate	Outer-rise/Near-trench reactivated mid-ocean fabric	Outer-rise/Near trench cross-cutting mid-ocean fabric	Intraslab High deformation (slab bends and dueling slabs)	Intraoceanic
Mechanism	Thrust	Normal	Normal	Normal	Strike-slip
Fault Maturity	High ← Low				

Although the range of apparent stress for teleseismically analyzable earthquakes is a continuum from less than 0.05 MPa up to 250 MPa, the outlier populations of earthquakes that radiate anomalously low or high amounts of energy are easily identifiable. The criteria stated in terms of apparent stress, slowness parameter Θ and differential magnitude ΔM are summarized in Table 2. These outlier populations have significant implications for tsunami

and seismic hazards evaluation, respectively. Slow earthquakes associated with transoceanic tsunamis have been characterized as having abnormally long source durations and anomalously low radiated seismic energy. On the other hand, the Mw of highly energetic earthquakes might belie the actual potential for damage from shaking. Figure 6 highlights three recent events (red stars) which inflicted considerable destruction or generated macroseismic effects. The ΔM´s of the Haiti 2010, Darfield, New Zealand 2010 and Christchurch, New Zealand 2011earthquakes range from 0.4 to 0.7. From these ΔM values we would rank their faults as immature and capable of higher seismic potential than their Mw alone would imply.

Table 2 Approximate relationship between apparent stress τ_a, slowness Θ, and differential magnitude ΔM. The relations are approximate as the value of shear modulus μ is a function of depth and earth structure. Thus, τ_a is influenced more by focal depth than Θ and ΔM.

	Slow tsunami earthquake	Enervated earthquake	Global average	High energy
τ_a	<0.1 MPa	< 0.1 MPa	0.5 MPa	≥ 1.0 MPa
Θ	< -5.5, Mw ≥ 7.5	< -5.5, Mw < 7.5	-4.9	≥ -4.6
ΔM (M_e-M_W)	< -0.5, Mw ≥ 7.5	< -0.5, Mw < 7.5	-0.2	≥ 0.0

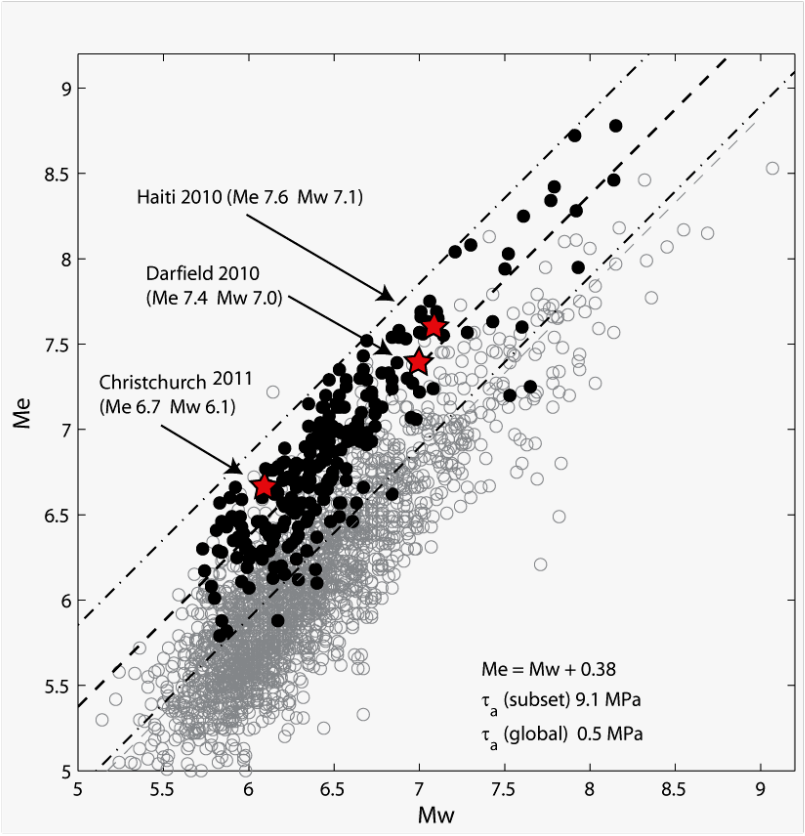

Figure 6 The red stars highlight some recent damaging earthquakes with Me >> Mw: the Haiti 2010, Darfield, New Zealand 2010 and Christchurch, New Zealand 2011 earthquakes. For comparison, global earthquake Me-Mw data are plotted as gray open circles and black closed circles show the subset of oceanic strike-slip earthquakes which are categorized as immature.

6 Summary

Modern magnitudes Mw and Me are direct measures of radiated energy and seismic moment, respectively. The amount of energy radiated per unit of seismic moment, representable in several ways such as differential magnitude ΔM and apparent stress τ_a, can be interpreted as an indicator of stress conditions in the lithosphere. Given the observed scatter in Me-Mw plots for the global earthquake population, no single empirical formula can accurately predict Mw from Me. However, the Mw and Me for subsets of earthquakes chosen on the basis of a specific tectonic setting, seismic region and focal-mechanism type occupy specific sectors of the Me-Mw plot. These patterns can be exploited to identify conditions of elevated seismic hazard, to identify conditions of elevated tsunami potential, and to be related to a model of fault maturity.

Acknowledgment

The author is deeply indebted to Dr. Peter Bormann for comprehensive comments and detailed suggestions that significantly improved the manuscript. The author also benefited from reviews by Drs. Domenico DiGiacomo, Emily So and Morgan Moschetti.

References

Abercrombie, R.E. and Ekström G. (2001). Earthquake slip on oceanic transform faults. *Nature*, **410**, 74-76.

Bormann, P., and D. Di Giacomo (2011). The moment magnitude M_w and the energy magnitude M_e: common roots and differences. *J. Seismology*, **15**, 411-427; doi: 10.1007/s10950-010-9219-2.

Bormann, P., Baumbach, M., Bock, M., Grosser, H., Choy, G. L., and Boatwright J. (2002). Seismic sources and source parameters in: Bormann, P. (ed), IASPEI *New Manual Seismological Observatory Practice*, GeoForschungsZentrum Potsdam, Vol. 1, Chapter 3, 94 pp.

Choy, G. L., and Boatwright, J. L. (1995). Global patterns of radiated seismic energy and apparent stress. *J. Geophys. Res.*, **100**, B9, 18,205-18,228.

Choy, G. L., Boatwright, J., and Kirby, S. (2001). The radiated seismic energy and apparent stress of interplate and intraslab earthquakes at subduction zone environments: Implications for seismic hazard estimation. *U.S. Geological Survey Open-File Report* **01-0005**, 18 pp.

Choy, G. L., and McGarr, A. (2002). Strike-slip earthquakes in the oceanic lithosphere: observations of exceptionally high apparent stress. *Geophys. J. Int.*, **150**, 506-523.

Choy, G. L., and Kirby, S. (2004). Apparent stress, fault maturity and seismic hazard for normal-fault earthquakes at subduction zones. *Geophys. J. Int.*, **159**, 991-1012.

Choy, G. L., and Kirby, S. H. (2009). Patterns in the spatial distribution of enervated and energetic subduction earthquakes based on broadband seismic wave-forms: Scientific Program of the USGS Tsunami Source Working Group, Menlo Park, CA.

Hanks, T. C., and Kanamori, H. (1979). Moment magnitude. *J. Geophys. Res.*, **84,** 2348-2350.

Kanamori, H., and Heaton, T. H. (2000). Microscopic and macroscopic physics of earthquakes. In: *GeoComplexity and the Physics of Earthquakes*, edited by J. B. Rundle, D. L. Turcotte, and W. Klein, Washington, D. C., AGU, 147–163.

Newman, A.V., and Okal, E.A. (1998). Teleseismic estimates of radiated seismic energy: The E/Mo discriminant for tsunami earthquakes. *J. Geophys. Res.*, **103**, 26885-26898.

Wyss, M., and Brune, J.N. (1968). Seismic moment, stress, and source dimensions for earthquakes in the California-Nevada regions. *J. Geophys. Res.*, **73**, 4681-4694.